

Genesis of the glaciotectonic thrust-fault complex at Halk Hoved, southern Denmark

TILLIE M. MADSEN & JAN A. PIOTROWSKI



Madsen, T. M. & Piotrowski, J. A. 2012. Genesis of the glaciotectonic thrust-fault complex at Halk Hoved, southern Denmark. © 2012 by Bulletin of the Geological Society of Denmark, Vol. 60, pp. 61–80. ISSN 0011–6297 (www.2dggf.dk/publikationer/bulletin).
<https://doi.org/10.37570/bgds-2012-60-05>

Received 24 November 2011
Accepted in revised form
26 September 2012
Published online
5 December 2012

The coastal cliff of Halk Hoved, southern Jutland, Denmark, is a major glaciotectonic complex formed by proglacial deformation of the North-East (NE) advance from the Scandinavian Ice Sheet in Late Weichselian. We describe and interpret the pre-, syn- and post-tectonic sedimentary successions and macro-scale architecture of this complex. Initially, the Lillebælt Till Formation (unit 1) and the overlying glaciofluvial sediments (unit 2) were deposited during the Warthe glaciation in Late Saalian. During the NE advance towards the Main Stationary Line (MSL) in Late Weichselian, these sediments were pushed along a décollement surface whereby a thrust-fault complex was formed. In a cross section the complex extends for more than 900 m and consists of eighteen c. 15–20 m thick thrust sheets stacked by piggyback thrusting. Accumulated displacement amounts to at least 235 m along thrust faults dipping at 30–40° towards N-NE, resulting in at least 24% glaciotectonic shortening of the complex. Deformation was presumably facilitated by elevated pore-water pressure in the Lillebælt Till Formation. As the compressive stress exceeded the shear strength of the weakened till, failure occurred, and a décollement horizon formed along the lithological boundary between the Lillebælt Till Formation and the underlying aquifer. During deformation, piggyback basins formed wherein sediments of hyperconcentrated flow (unit 3) and glaciolacustrine diamicton (unit 4) were deposited. The whole thrust-fault complex and the intervening sediments were truncated subglacially as the NE advance finally overrode the complex. Following the retreat of the NE advance, a succession of glaciofluvial sediments (unit 5) and finally the East Jylland Till Formation (unit 6) were deposited during the advance of the Young Baltic Ice Sheet. The Halk Hoved thrust-fault complex is a prominent example of glaciotectonism at the southern fringe of the Scandinavian Ice Sheet.

Keywords: Glaciotectonism, thrust-fault complex, pore-water pressure, lithostratigraphy.

Tillie M. Madsen [tmm@ramboll.dk], Rambøll Danmark A/S, Olof Palmes Allé 22, DK-8200 Aarhus N, Denmark. Jan A. Piotrowski [jan.piotrowski@geo.au.dk], Department of Geoscience, Aarhus University, Høegh-Guldbergs Gade 2, DK-8000 Aarhus C, Denmark.

Glaciotectonic deformation is a common phenomenon in Denmark (Jakobsen 1996, 2003). During the Pleistocene multiple ice sheet advances over Denmark generated large glaciotectonic complexes in which sediments were deformed by folding and/or displaced along thrust faults. These ancient glaciotectonic complexes, as well as modern complexes found along ice margins of present-day glaciers, provide information about the glaciodynamics and environmental conditions at the ice sheet margins. The purpose of this paper is to present the spatial and sedimentological

characteristics and a model of formation of the prominent Late Pleistocene glaciotectonic complex exposed along the coastal cliff of Halk Hoved in the southern part of Denmark. The study comprises an examination of pre-, syn- and post-tectonic sedimentary successions and large-scale architecture of the glaciotectonic structures, and a genetic interpretation of the entire complex. Furthermore, by comparing with other well known glaciotectonic features we discuss the factors that played a key role in the formation of the Halk Hoved complex.

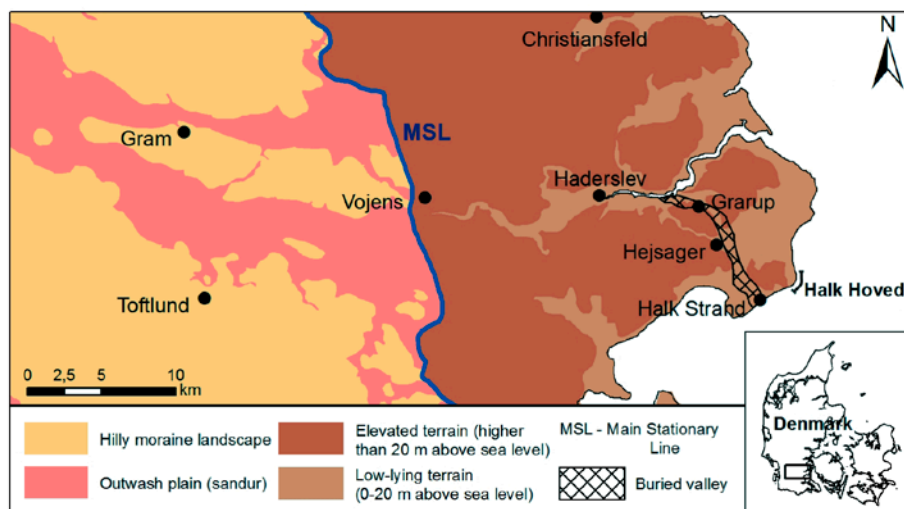


Fig. 1. Map showing the location of Halk Hoved and the surrounding landscape. The Main Stationary Line is drawn on the basis of Smed (1981).

Study area and geological setting

The coastal cliff Halk Hoved is located along the eastern coast of the southern part of Jutland approximately 12 km southeast of Haderslev (Fig. 1). The cliff face is approximately 900 m long and 10–20 m high and is generally well exposed due to high sea erosion rates and mass movement. The large-scale architecture of the cliff and its sediments has previously been investigated by Jessen (1930, 1935), Frederiksen (1975, 1976) and Houmark-Nielsen (1987). At Halk Hoved there is evidence of two glaciations: the Saalian and the Weichselian glaciation. During Late Saalian and Weichselian the area was overridden by several ice advances of the Scandinavian Ice Sheet. In Late Saalian, the ice sheet advanced through the Baltic depression and deposited the Lillebælt Till Formation (Warthe glaciation; c. 150–130 kyr ago) (ICS 2010). After the Eemian Interglacial the area underwent a long period of periglacial conditions that was briefly interrupted in Middle Weichselian by ice sheets advancing through the Baltic depression (Ristinge glaciation; c. 55–50 kyr ago) during which the Ristinge Klint Till Formation was deposited (Houmark-Nielsen 2007). In Late Weichselian (c. 25 kyr ago) during the Last Glacial Maximum (LGM) the area was covered by an ice sheet from Sweden referred to as the North-East (NE) advance that deposited the Mid Danish Till Formation (Houmark-Nielsen 2007). The NE advance had an extended period of ice-marginal standstill at the Main Stationary Line (MSL), approximately 20 km west of Halk Hoved (Fig. 1), where the landscape changes abruptly from a hilly terrain to a flat sandur plain that encloses older moraine hills (Kjær *et al.* 2003, Houmark-Nielsen 2007). During the subsequent Young Baltic advance (c. 19 kyr ago) the ice sheet passed through the Baltic depression and deposited

the East Jylland Till Formation (Houmark-Nielsen 2007) which is the youngest glacial deposit in the study area. The Weichselian glaciers shaped the landscape surrounding Halk Hoved into hilly moraine plateaus that are traversed by E–W and SSE–NNW oriented valleys.

Methods

During field work, serial sketches were drawn of the cliff faces at a scale of 1:100, recording the large-scale geometry of the lithofacies and glaciotectionic structures. The general architecture of the macro-scale glaciotectionic structures was described and recorded by measuring the orientation (strike and dip) of folds, faults and bedding planes. The lithofacies were described and classified according to the scheme by Krüger & Kjær (1999). Each lithofacies was described in terms of lithology, grain size, sedimentary structures, and main characteristics, and assigned a lithofacies code.

Additional descriptive information was provided for diamicton and glaciofluvial facies by analysing the granulometric and petrographical composition. Samples were collected at different intervals along the cliff face. The granulometric composition was determined by sieve and pipette methods and is graphically presented by the weight percentage for each size class. The grain-size distribution was defined within the range of 0.001 mm to 4 mm, limited by the sample volume.

The petrographical composition was determined for the fine-gravel fraction (2–4 mm) after Kronborg (1986) and Kronborg *et al.* (1990). The fine-gravel fraction was divided into two main groups according

to their stability against chemical weathering, viz. a stable and an unstable group (Kjær *et al.* 2003). The stable group with at least three hundred identified grains per sample was classified into crystalline rocks, quartz, flint and sedimentary rocks, while the unstable group was classified into Cretaceous–Danian limestone and Palaeozoic limestone. In accordance with Ehlers (1979) each stable subgroup (crystalline, quartz, flint and sedimentary rocks) is calculated as a percentage of the sum of stable grains, so that the stable group is depicted as 100% in diagrams. The unstable subgroups (Cretaceous–Danian limestone and Palaeozoic limestone) are calculated separately as a percentage of the sum of stable grains and are in diagrams expressed as a percentage of the stable group. Both the granulometric and petrographical composition were used to define and distinguish lithostratigraphical units.

Lithostratigraphy

In the Halk Hoved cliff section six lithostratigraphical units were recognised. The two lowermost units (unit 1 and 2) were subjected to macro-scale deformation. Unit 2 is overlain by an erosional unconformity upon which lithostratigraphical units 3 and 4 were deposited. The whole assemblage of units 1–4 is truncated by a glaciotectionic unconformity, whereupon lithostratigraphical unit 5 is deposited. This is in turn overlain by an erosional unconformity and the laterally extensive unit 6. Fig. 2 shows the large-scale architecture and the lithofacies geometry of the Halk Hoved cliff section. A simplified log of the lithostratigraphical units is presented in Fig. 3.

Unit 1

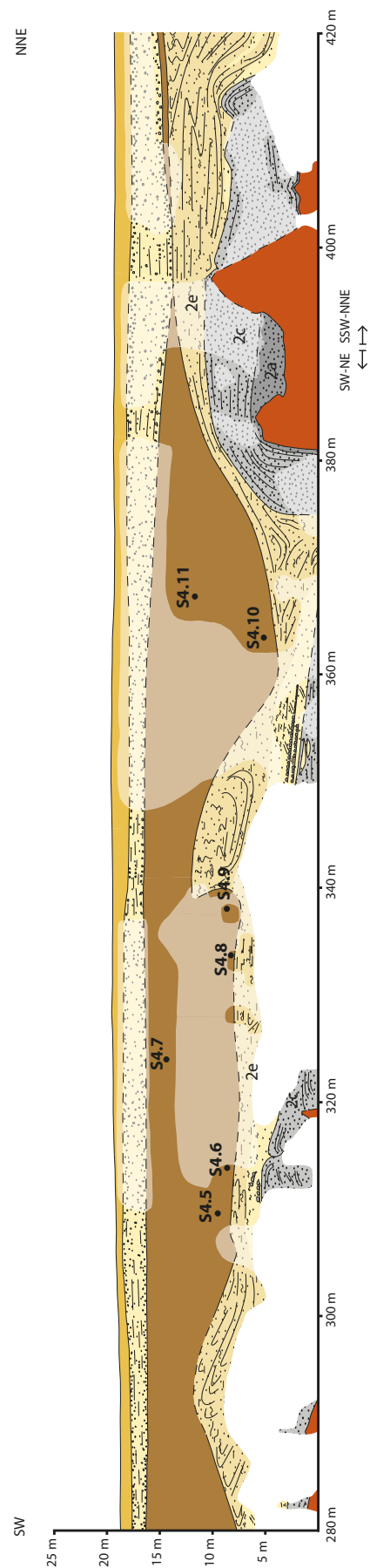
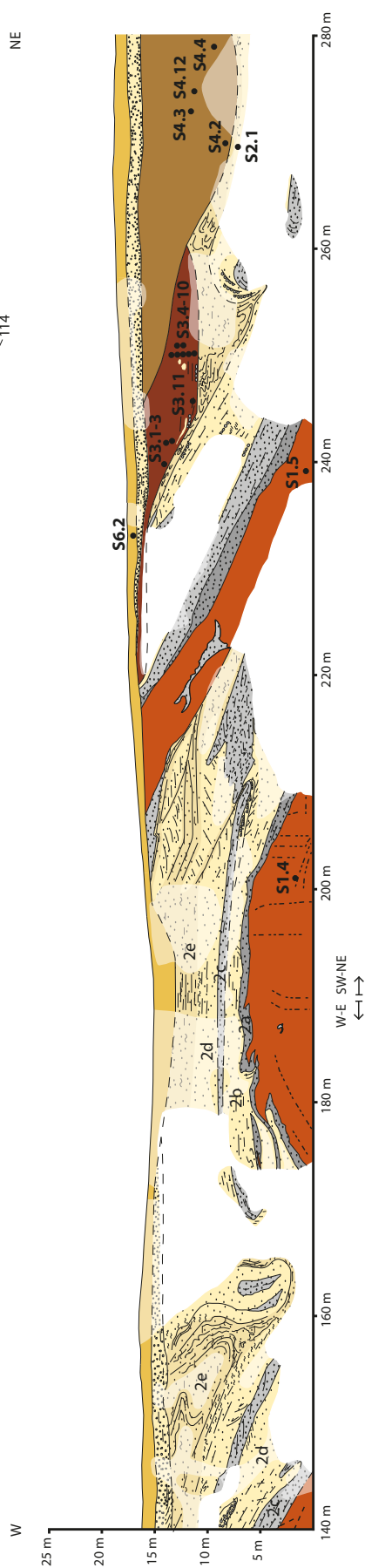
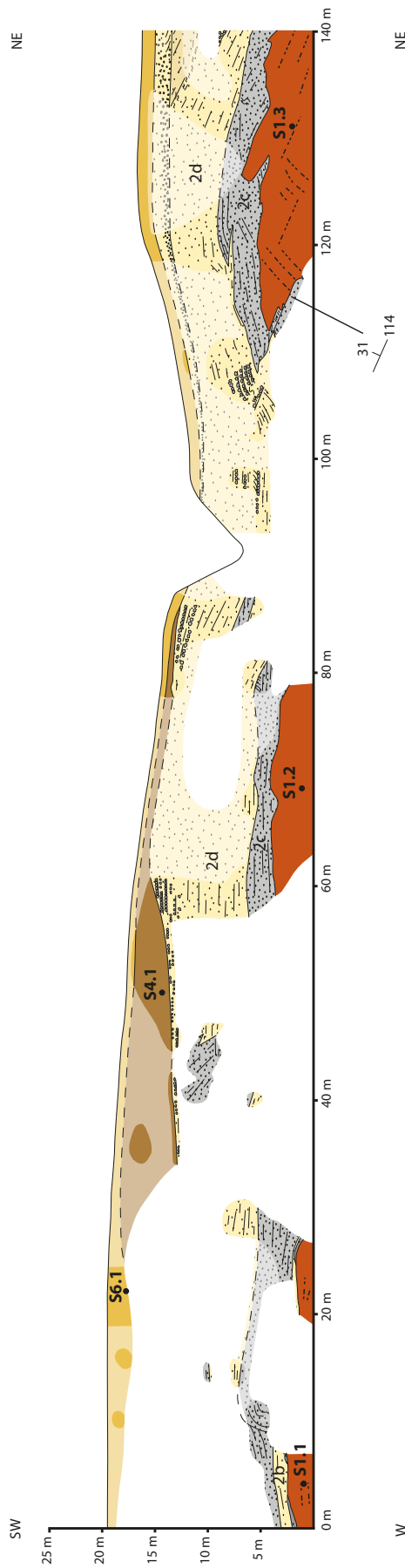
Unit 1 is a grey, fine-grained (clayey-silty), matrix-supported diamicton with a moderate content of clasts. In general, the diamicton is characterised by a firm, massive, homogeneous structure (DmF(m₂)/3). Only few structural elements have been observed, such as a 2–3 cm thick, heavily tectonized, silty string of sand, a small lens of gravel, and a relatively large displaced gravel lens (between points 117 m and 225 m on Fig. 2). The diamicton has a minimum thickness of 4 m and is traversed by subvertical and subhorizontal fissures. On average, the matrix of the diamicton contains 36% sand (σ 2.3%; σ is the standard deviation), 43% silt (σ 2.5%), and 21% clay (σ 2.1%) (Fig. 3). The matrix is characterised by a bimodal grain-size distribution with a primary mode in fine sand and a secondary mode in fine silt (Fig. 4). The petrographical composition is on

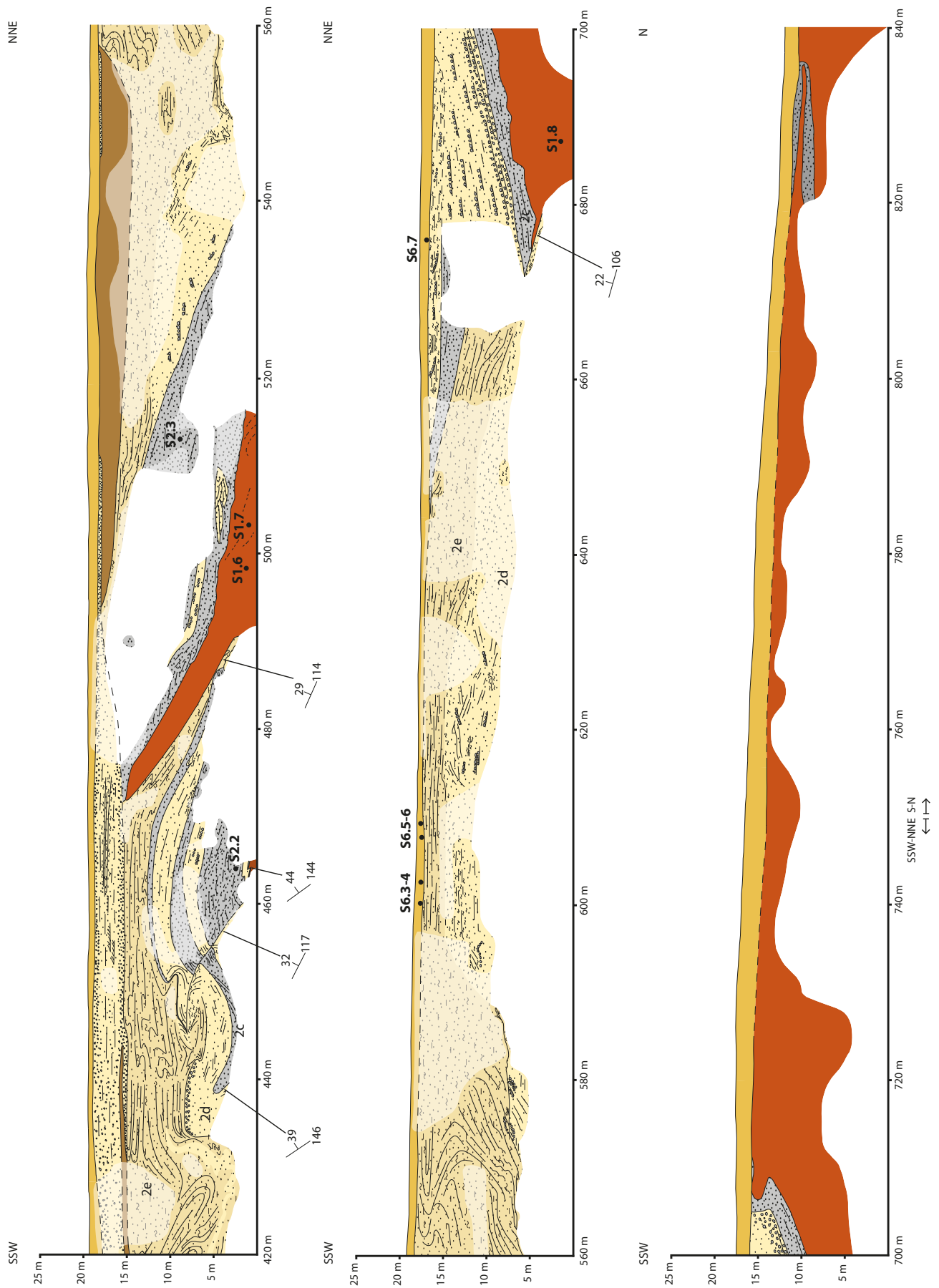
average 67% crystalline rocks (σ 3.0%), 7% quartz (σ 1.2%), 20% flint (σ 2.7%), and 6% sedimentary rocks (σ 2.0%) (Fig. 3). The unit is also characterised by a relatively high content of both Cretaceous–Danian limestone (32%; σ 5.5%) and Palaeozoic limestone (38%; σ 6.1%).

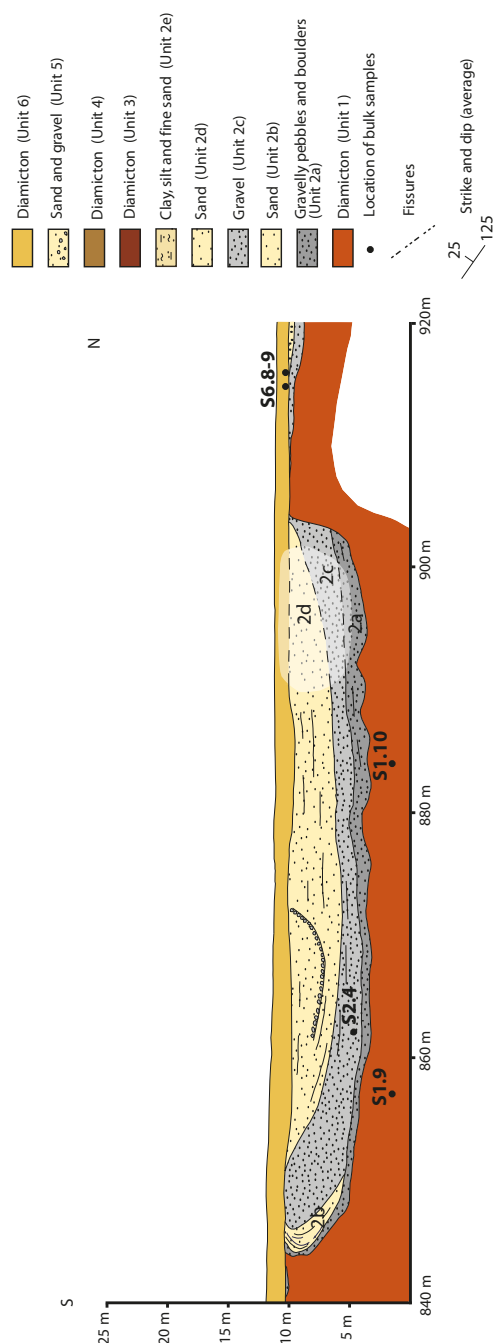
Unit 1 is interpreted as a subglacial till. The interpretation is consistent with the granulometric composition, since subglacial tills commonly show bi- and polymodal grain-size distributions as a result of comminution during which particle sizes are reduced through crushing and abrasion (Dreimanis & Vagners 1971; Boulton 1978; Haldorsen 1981, 1983; Piotrowski 1992; Larsen *et al.* 2004; Piotrowski *et al.* 2006). Depositional processes may have included lodgement, deformation, clast ploughing and the development of a liquefied till layer, and the unit is therefore classified as a subglacial traction till *sensu* Evans *et al.* (2006).

Unit 2

Unit 2 overlies unit 1 with a sharp, erosive contact. It forms a fining-upward succession of glaciofluvial sediments consisting of five facies (unit 2a–2e) with a total thickness of 6–12 m. The first facies (unit 2a) consists of localised clusters of open-work to matrix-supported, massive, angular to rounded boulders and gravelly pebbles (B) with a general thickness of 0.3–1.5 m. It is overlain by a facies (unit 2b) comprising discontinuous, thin sheets (c. 1 m thick) of coarse- to medium-grained sand that are massive (Sm), horizontally bedded (Sh), and cross-bedded (Sp). Unit 2b is overlain by unit 2c which consists of laterally extensive, stacked sheets of massive (Gm) and horizontally bedded (Gh), clast- to sand-supported, imbricated gravel. The thickness of unit 2c is 1–4 m. It is succeeded by a sandy facies (unit 2d), the thickness of which varies greatly from 2 to 10 m. This facies consists of coarse- to medium-grained sand that is massive (Sm), horizontally bedded (Sh) and trough cross-bedded (St), with intercalations of massive gravel (Gm). Upward, the sand becomes medium- to fine-grained and exhibits trough cross-bedding (St) and horizontal bedding (Sh) with intercalations of silt flasers (Fm). As unit 2d gradually turns into unit 2e the silt flasers become more pronounced, so that unit 2e consists of massive (Fm) and laminated silty clay (Fl) with intercalations of laminated (Sh) and cross-laminated (Sr) fine-grained sand. Unit 2e is heavily contorted by open and overturned folds due to ductile deformation. The thickness of unit 2e varies greatly in relation to the degree of deformation. When the sediment is heavily deformed the thickness can be up to 8 m due to tectonic repetition and superimposition, while a more or less undisturbed sediment has a thickness around 2 m.







◀▲ Fig. 2. Halk Hoved cliff section as mapped in 2005 and 2006. The 'faded' colours represent interpreted areas. The different subunits of unit 2 (2a-2e) are shown on the cross section. Bulk samples at different intervals along the cliff face were taken for granulometric and petrographical analyses of the lithostratigraphic units 1, 3, 4 and 6. Additional samples were taken from unit 2c and 2d for petrographical analysis. The location of samples is shown in the profile. A sample named S1.3 means sample 3 from unit 1.

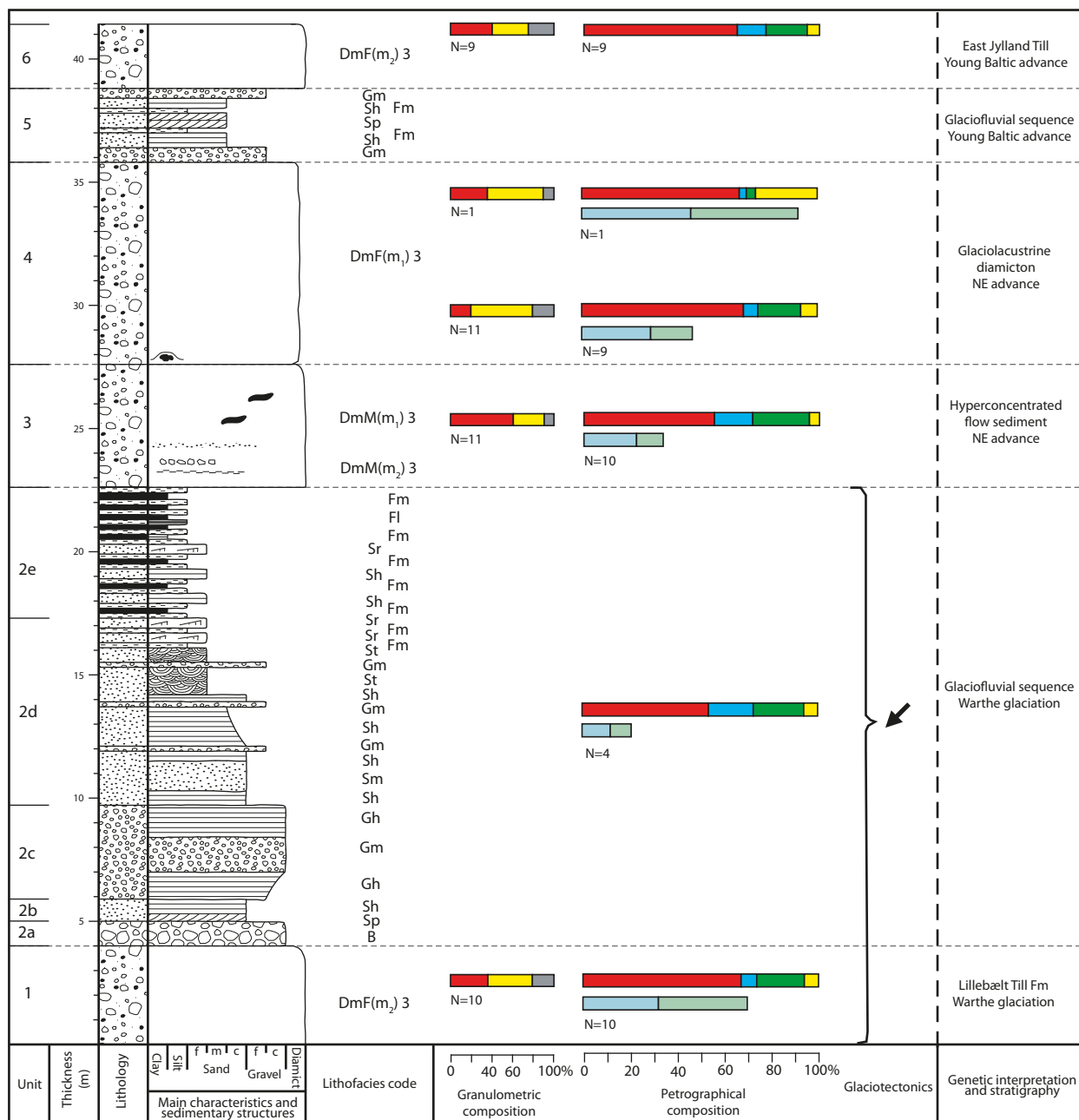
The petrographical composition of the glaciofluvial sediment shows an average fine-gravel content of 54% crystalline rocks (σ 7.1%), 19% quartz (σ 4.9%), 21% flint (σ 7.6%) and 6% sedimentary rocks (σ 1.5%), and in the unstable group of 12% Cretaceous–Danian limestone (σ 5.8%) and 9% Palaeozoic limestone (σ 3.8%) (Fig. 3). This fining-upward succession of glaciofluvial sediments reflects the change from a proximal to a distal glaciofluvial environment likely due to a receding ice margin.

Unit 3

Unit 3 is a brown, massive, compact, medium-grained (silty–sandy) diamicton. The matrix consists of 61% sand (σ 1.8%), 30% silt (σ 1.7%) and 9% clay (σ 1.7%) and is characterised by a unimodal grain-size distribution with a mode in medium-grained sand (Fig. 4). The gravel content is moderate (DmM(m_2)3) but seems to diminish upward (DmM(m_1)3), primarily within the lowermost 1.5 m. The diamicton contains a few structural elements such as sand lenses, a string of laminated fine-grained sand and silt, and a layer of massive gravel (Fig. 5a and b). Furthermore, the lower part of the sediment is stratified, with small, no more than 1 cm thick, grey, clayey laminae. These interbedded layers of sorted sediment are parallel to the basal contact of the unit. Unit 3 is only observed in the cliff section at 220–260 m, where it lies discordantly over the deformed assemblage of unit 1 and 2 (Fig. 2). The thickness of unit 3 increases towards north from c. 0.5 m to a maximum of 5 m, after which it thins into a wedge. The lower boundary of the sediment is very sharp and along its base small overturned folds (drag folds) are observed in the underlying glaciofluvial clay and silt (unit 2e).

Unit 3 has a petrographical composition with 56% crystalline rocks (σ 3.0%), 16% quartz (σ 2.6%), 24% flint (σ 2.9%), 4% sedimentary rocks (σ 1.7%); 22% Cretaceous–Danian limestone (σ 5.4%) and 11% Palaeozoic limestone (σ 1.8%) (Fig. 3).

Unit 3 is interpreted as deposited from a hyperconcentrated flow. A hyperconcentrated flow was originally defined by Beverage & Culbertson (1964) as a subaerial turbulent flow that in the rheological terms of flow behaviour is transitional between normal stream flow and debris flow. It is characterised by a suspended sediment concentration that exceeds 25% by volume (Mulder & Alexander 2001). The suspended material is a mixture of two populations; one in the sand fraction and the other in the silt-clay fraction (Beverage & Culbertson 1964), which is consistent with the granulometric composition of unit 3. The clay content is generally very low because a hyperconcentrated flow is a friction-dominated non-cohesive flow (Mulder & Alexander 2001).



Lithofacies code (Krüger & Kjær 1999)

Diamict sediments	Sorted sediments
D Diamict	B Boulders
m Massive, homogeneous	Gm Gravel, massive
M Medium-grained, silty-sandy	Gh Gravel, horizontally bedded
F Fine-grained, clayey-silty	Sm Sand, massive
(m ₁) Matrix-supported, clast poor	Sh Sand, horizontally laminated
(m ₂) Matrix-supported, moderate clast content	St Sand, trough cross-bedded
3 Firm, difficult to excavate	Sp Sand, planar cross-bedded
	Sr Sand, ripple cross laminated
	Fm Fines (silt, clay), massive
	Fl Fines (silt, clay), laminated

Glaciotectionics

Estimated direction of glaciotectionic deformation

Other sedimentary structures

- Drop stone draped by lamina
- Lenses of sand
- Horizon of clay/silt, sand or gravel

Average granulometric composition [%]

Sand Silt Clay
N=number of samples

Average petrographical composition [%]

Crystalline rocks Quartz Flint Sedimentary rocks Limestone (Cretaceous-Danian) Palaeozoic limestone
N=number of samples

Fig. 3. The glacio-stratigraphic section of Halk Hoved. The diagram shows a lithostratigraphical log accompanied by the average granulometric and petrographical composition for units 1, 3, 4 and 6. The average petrographical composition of unit 2c and 2d is also shown. The sedimentary units are described and classified using lithofacies codes in accordance with the scheme by Krüger & Kjær (1999).

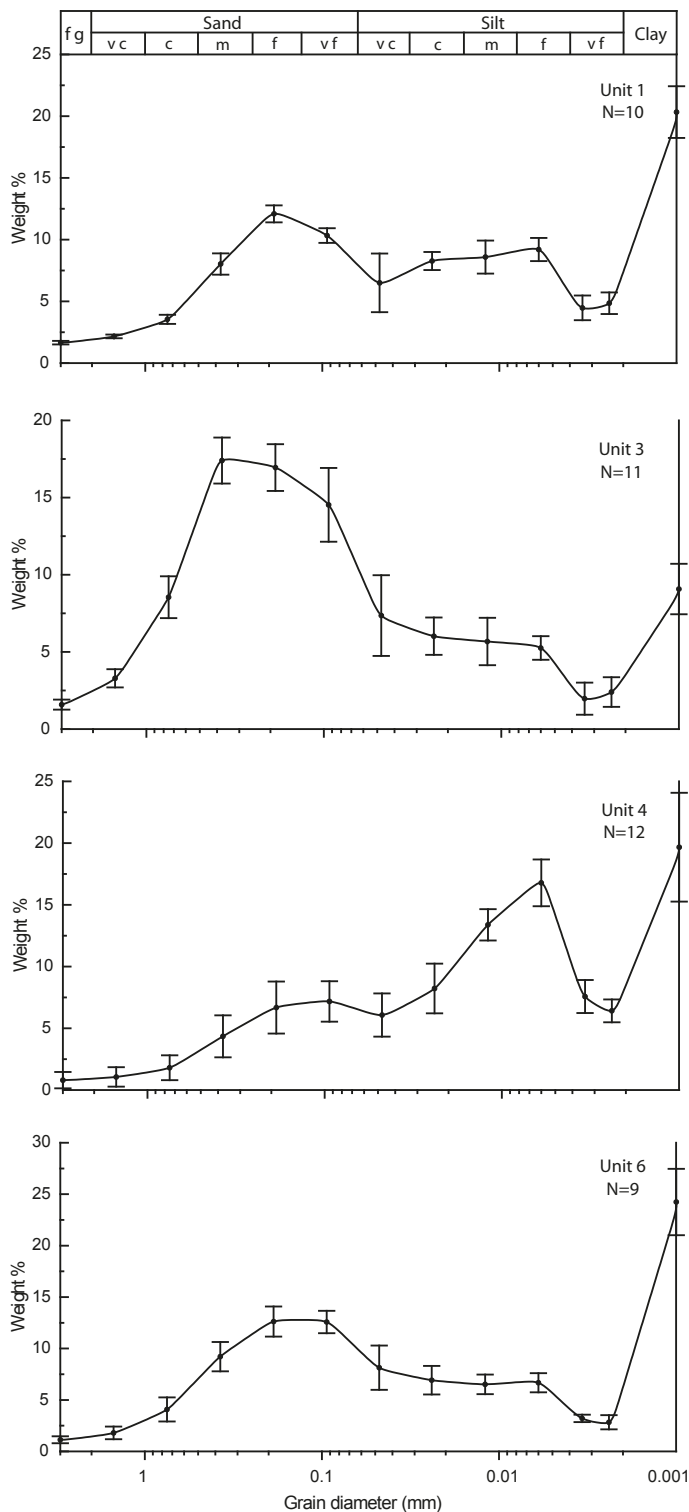


Fig. 4. Grain size distribution with standard deviations (vertical bars are $\pm 1\sigma$) from units 1, 3, 4 and 6. The abbreviations denote fine gravel (fg), very coarse (vc), coarse (c), medium (m), fine (f) and very fine (vf).

Hyperconcentrated flows occur either due to mass movement or water action eroding and remobilising sediment. With regard to unit 3, the hyperconcentrated flow was likely initiated by the mobilisation of glaci-ofluvial material (unit 2) down a slope. Presumably, mobilisation was prompted by high pore-water pressures reducing the frictional strength of the sediment, giving the sediment little resistance to downslope movement. The main depositional mechanism would have been frictional freezing from grain-to-grain interaction. This would have triggered rapid dumping of the suspended material, thereby preventing deposition from traction (Bilka & Nemec 1998; Mulder & Alexander 2001) and resulting in the massive structure of unit 3. The few structural elements observed within unit 3 are interpreted to be the result of resedimentation by water, indicating that deposition occurred by the accretion of successive flow surges (Sohn *et al.* 1999).

Unit 4

Unit 4 has been observed in the cliff section at 30–90 m, 250–440 m, and 490–560 m, discordantly overlying deformed sediments (Fig. 2). It is a blackish grey, compact, massive, fine-grained (clayey-silty), matrix-supported diamicton with a low content of clasts (DmF(m)₃) and a small content of dispersed stones (Fig. 5c). The unit has a very variable thickness ranging between 2 and 13 m. The only structural elements observed are a clayey lamina draped over a stone, and layers of sand and gravel. The lower contact is sharp, and in a few places the lowermost 1 m of the sediment is more compact than the rest and has a reddish colour. The matrix of unit 4 consists on average of 21% sand (σ 5.4%), 59% silt (σ 3.9%) and 20% clay (σ 3.3%) (Fig. 3) and is characterised by a bimodal grain-size distribution with a very distinct primary mode in fine silt and a secondary mode in very fine sand (Fig. 4). The fine-gravel composition is 69% crystalline rocks (σ 2.7%), 6% quartz (σ 1.5%), 18% flint (σ 2.5%), 7% sedimentary rocks (σ 1.7%); 32% Cretaceous–Danian limestone (σ 10.5%) and 20% Palaeozoic limestone (σ 1.4%) (Fig. 3).

Towards the upper contact, the matrix of unit 4 becomes slightly more coarse-grained and consists of 36% sand, 54% silt and 10% clay (Fig. 3; sample S4.7 in Fig. 2). Here, the massive sediment has a yellow-brown colour and is interbedded with limestone clasts. Furthermore, the petrographical composition also differs from the rest of unit 4 by having much less flint and a higher content of limestone; the composition is 67% crystalline rocks, 3% quartz, 4% flint, 26% sedimentary rocks; 46% Cretaceous–Danian limestone and 46% Palaeozoic limestone. Due to limited access, it is uncertain whether it is only a localised or a more

widespread phenomenon or even if this sediment represents a similar depositional environment as the rest of unit 4.

Unit 4 is interpreted as a glaciolacustrine diamicton. The deposition of glacial diamicton in an ice-contact lake is often attributed to iceberg calving with a subsequent debris rainout (Domack & Lawson 1985; Dowdeswell *et al.* 1994; Bennett *et al.* 2002) and/or subaqueous sediment gravity flows (Evenson *et al.* 1977; May 1977; Rovey & Borucki 1995) that receive its material from a subglacially deforming bed at the grounding line (Benn 1996; Bennett *et al.* 2002). The massive structure of unit 4 suggests that during deposition the sedimentation rates must have been high in order to suppress structures such as lamination. The very faint clayey lamina draped over a stone represents a period with stagnant water and low sediment supply during which fallout from suspension could occur.

Unit 5

Unit 5 consists of a discontinuous, 1–4 m thick glaciofluvial succession made up of massive gravel (Gm) interbedded with horizontally bedded (Sh) and cross-

bedded (Sp) medium- to fine-grained sand with intercalations of silt flasers (Fm). The unit is interpreted to have been deposited in a glaciofluvial environment with massive gravel representing migrating longitudinal bars and the sand representing migrating sandy bedforms (Miall 1985). The massive gravel indicates high-energy water flows that were interrupted by periods of low-energy water flow during which the sandy bedforms were deposited.

Unit 6

The whole cliff is draped by a continuous, brown-coloured, fine-grained (clayey-silty) diamicton with an almost uniform thickness around 1–2 m. The diamicton is massive, firm and matrix-supported with a moderate content of clasts (DmF(m₂)₃). It is characterised by a sharp basal contact and fissile structure with some sand and silt strings. The uppermost 0.5 m is disturbed by post-depositional weathering and modern farming activities.

Unit 6 has a petrographical composition of on average 65% crystalline rocks (σ 2.0%), 12% quartz, (σ 1.5%) 18% flint (σ 2.0%) and 5% sedimentary rocks (σ 0.9%)

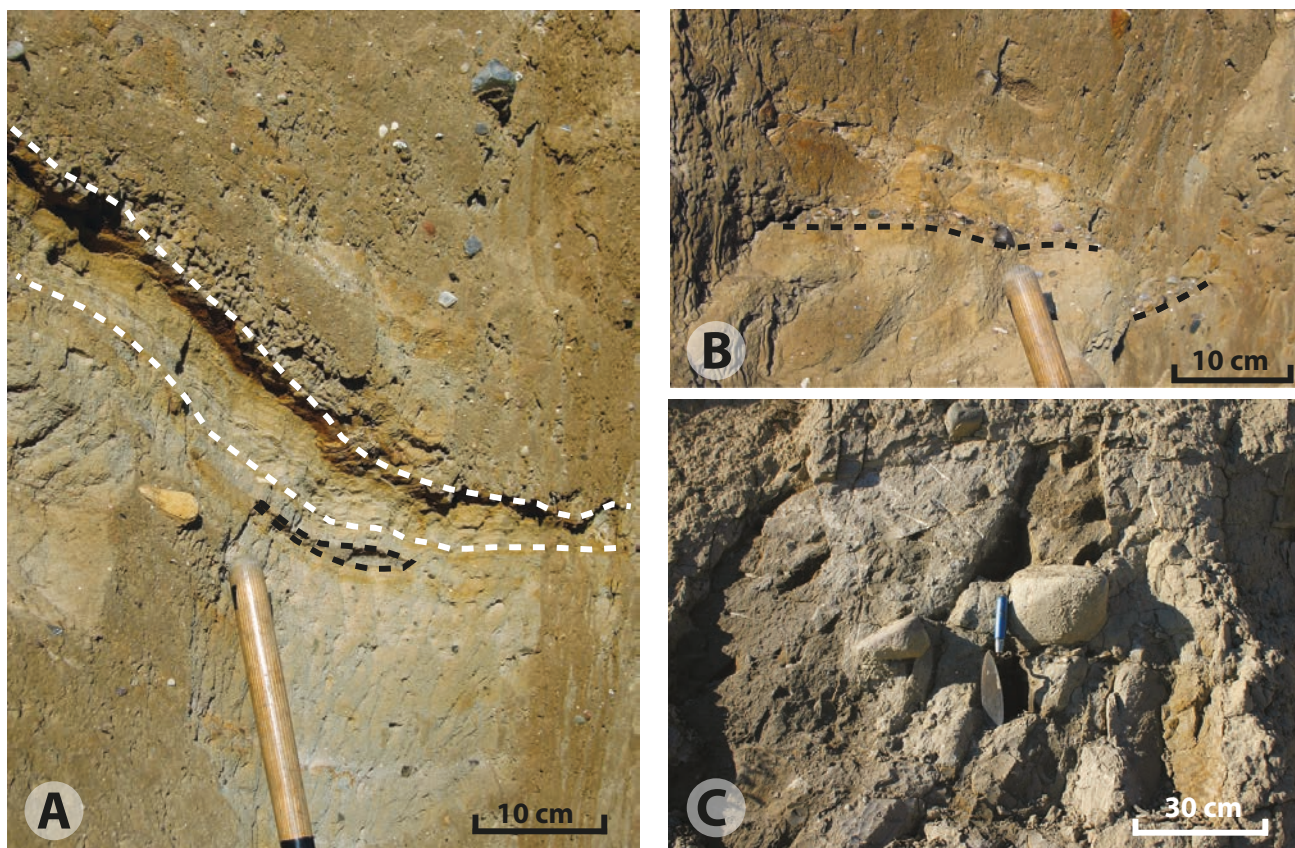


Fig. 5. **A**, Layer of laminated sand and silt interbedded in medium-grained diamicton of unit 3, marked by the white dashed line. Underneath the layer there is a small stretched-out lens of coarse-grained sand indicated by the black dashed line. **B**, Thin layer of gravel resting within medium-grained diamicton of unit 3, underlined by the two black dashed lines. **C**, Blackish grey, compact, massive, clayey silt deposit (unit 4) with two dropstones on both sides of the spatula.

(Fig. 3). The matrix consists of 40% sand (σ 3.6%), 35% silt (σ 3.5%) and 25% clay (σ 3.2%) (Fig. 3), and, like unit 1, the matrix is characterised by a bimodal grain-size distribution with a primary mode in fine sand and a secondary mode in fine silt (Fig. 4). The only difference between the two sedimentary units is that unit 6 is slightly more coarse-grained.

Like unit 1, unit 6 is interpreted as a subglacial traction till (Evans *et al.* 2006). Lodgement was presumably the main depositional process, but subglacial deformation and/or the development of a liquefied till layer would likely also have occurred, particularly in areas where this unit is lying directly over unit 4 and unit 2d, as the low permeability of these sediments would have facilitated high pore-water pressures.

Structural analysis of the glaciotectonic complex

In the following a structural description of the glaciotectonic elements exposed at the Halk Hoved cliff is given with preliminary interpretations to facilitate the understanding of the deformational framework. The macro-scale tectonic structures are described using the terminology associated with thin-skinned thrust-fault tectonics (i.e. footwall, hanging-wall, ramp, and flat). For a detailed description of these terms see Pedersen (2005).

The glaciotectonic complex is divided into two subsections: a distal deformation zone comprising the cliff section at 0–600 m, and a proximal deformation zone comprising the cliff section at 600–920 m. Within the distal deformation zone sixteen thrust sheets are identified, whereas only two thrust sheets are recorded in the proximal zone. In general, the thrust sheets are composed of a diamicton (unit 1) overlain by a varied succession of glaciofluvial sediments (unit 2a–2e). The interpreted architecture of the thrust sheets is shown in Fig. 6.

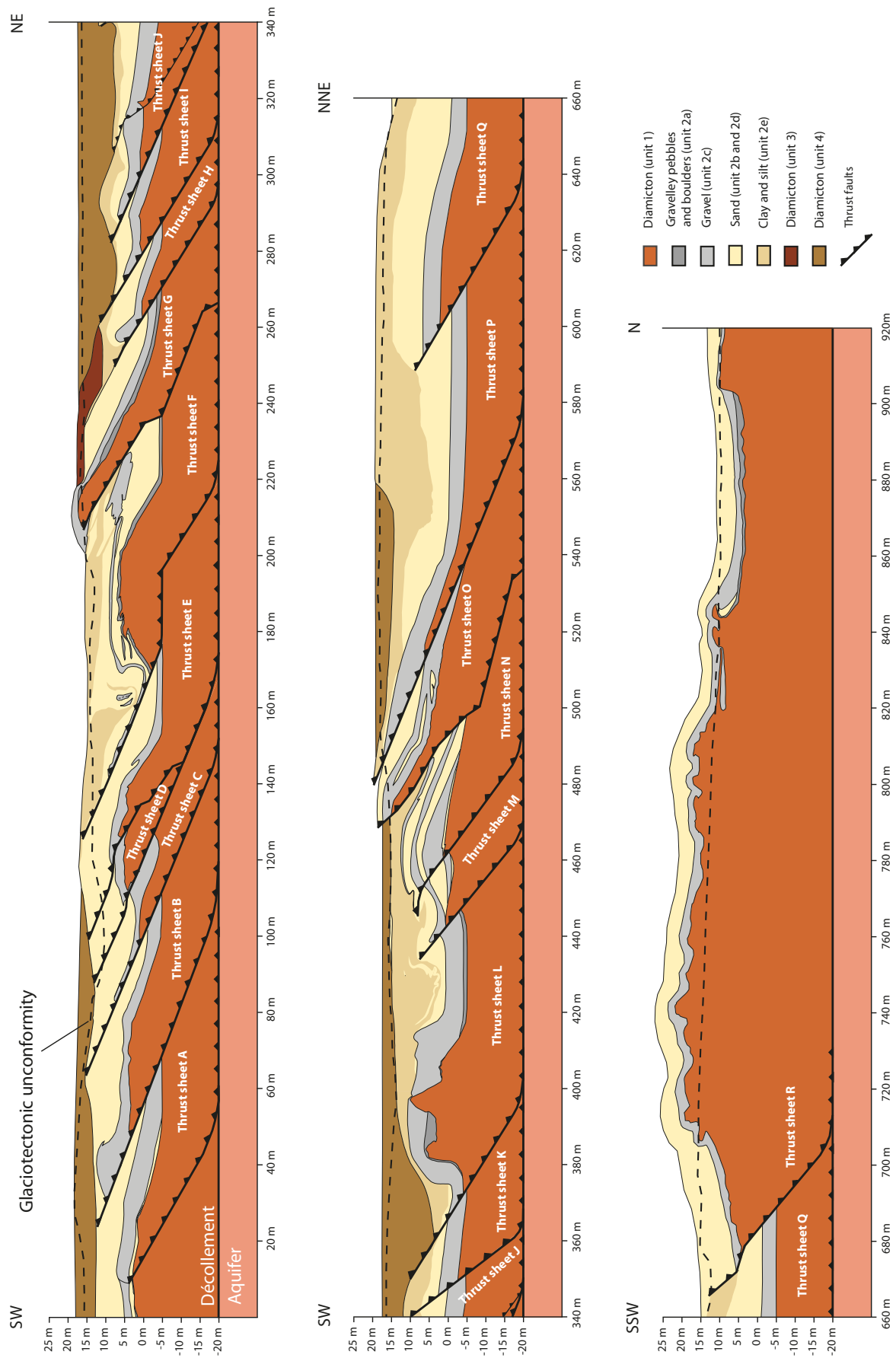
The exposure in the first 100 m of the southern end of the cliff constitutes the most distal part of the glaciotectonic complex. It is somewhat obscured by vegetation which also covers the contact to the foreland (Fig. 2). Two flat-lying thrust sheets (A and B) are inferred from divergent bedding directions observed within the gravel (unit 2c) and sand (unit 2d) (Fig. 6). Thrust

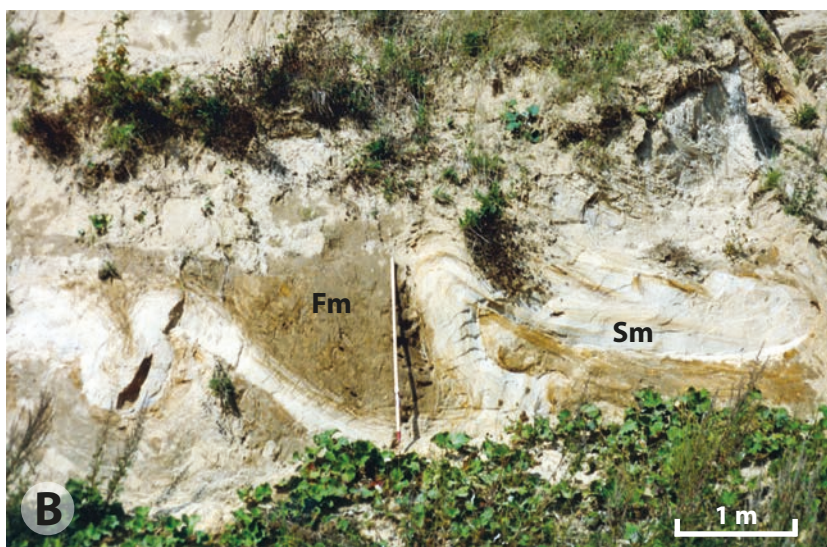
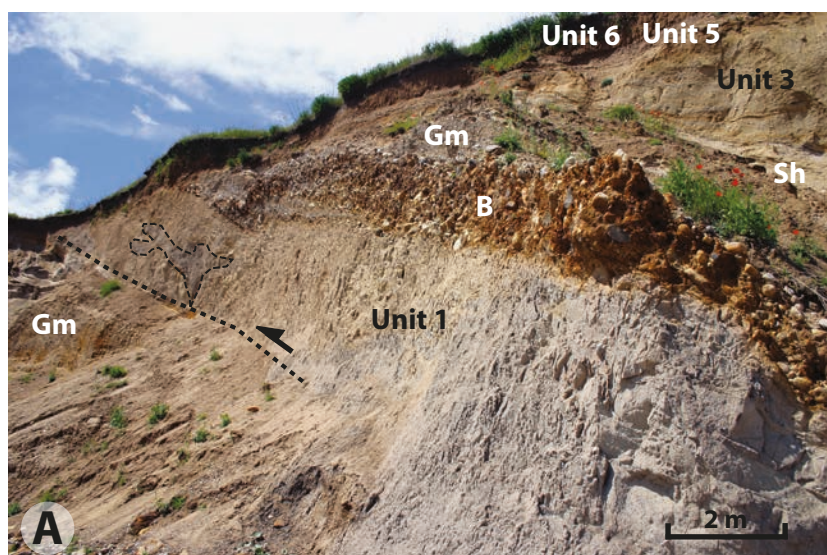
sheet A is about 15 m thick and is composed of unit 1 overlain by a succession of unit 2a–2d. The frontal part of the thrust sheet is defined by a footwall ramp at point 10 m along which thrust sheet A has been displaced for about 1–2 m. During the displacement a fault-propagation fold developed in the hanging-wall of thrust sheet A, causing the bedded gravel (unit 2c) to be folded (Fig. 2). The fold developed because the propagating thrust sheet lost slip towards the tip of the fault, and the lack of slip was then compensated by folding (Brandes & Le Heron 2010). The trailing end of thrust sheet A is truncated by thrust sheet B at point 55 m. Thrust sheet B is approximately 15 m thick and consists of unit 1 with an overlying succession of unit 2c–2b. Unit 4 was deposited on top of the crest of the thrust sheet (Fig. 6). The gravel layer (unit 2c) located between points 40 m and 47 m outlines a hanging-wall anticline at the frontal edge of the thrust sheet. The thrust sheet is estimated to have been displaced approximately 17 m.

Between points 80 m and 90 m, a 1 m thick layer of gravel (unit 2c) is seen up-thrust into the overlying sand (unit 2d), generating divergent bedding directions (Fig. 2). On the basis of the squeezed displacement of the gravel layer it is inferred that the *c.* 7 m thick thrust sheet C was displaced approximately 13 m on top of thrust sheet B (Fig. 6). At its trailing end, thrust sheet C is folded into a footwall syncline, causing the tilting of horizontally bedded sand between points 100 m and 110 m (Fig. 2). The footwall syncline is cut by a thrust fault dipping *c.* 31° NE. The thrust fault forms a footwall ramp along which the *c.* 6 m thick thrust sheet D was displaced about 17 m. The thrust fault is identified in the overlying sand (unit 2d) as a 2–3 cm thick, gravelly clay layer.

Thrust sheet E was displaced about 9 m over the footwall of thrust sheet D. Initially, the two thrust sheets constituted one thrust sheet, which became internally divided by a thrust fault separating it into two individual thrust sheets. During the propagation of thrust sheet E an upper footwall ramp developed, resulting in the formation of a hanging-wall anticline seen at point 135 m (Fig. 6). Within unit 1 several fissures developed during displacement of thrust sheet D and E. Some of the fissures (at point 140 m) show similar orientation as the fault beneath thrust sheet D, while others (at point 118 m) are more or less orientated perpendicular to the strike of the thrust fault (Fig. 2).

► Fig. 6. Interpreted large-scale glaciotectonic structures at Halk Hoved. The black dashed line at the top of the cross section represents the glaciotectonic unconformity, whereas the black dashed line between unit 1 and the underlying aquifer indicates the décollement plane. A reconstruction of the top of the thrust-fault complex (prior to erosion) is shown above the glaciotectonic unconformity. The unexposed area below the décollement plane is interpreted to constitute glaciofluvial sand deposits based on wells located inland west of the profile.





B Boulder Sm Sand, massive Fm Fines (silt, clay), massive
 Gm Gravel, massive Sh Sand, horizontally laminated

Fig. 7. **A**, The steeply dipping thrust sheet G composed of a diamicton (unit 1) overlain by a succession of B, Gm and Sh from unit 2. The thrust sheet is discordantly overlain by brown, silty diamicton of unit 3 seen in the upper right corner of the picture. Unconformably overlying thrust sheet G and unit 3 is a layer of gravel and sand (unit 5) followed by the upper diamicton (unit 6). Towards the left a displaced lens of massive gravel is interbedded in unit 1. Around 210–240 m in the profile. **B**, An overturned fold of fine-grained sand within unit 2e located between points 427 m and 433 m. **C**, Thrust sheet O composed of a wedge of diamicton (unit 1) and gravel (Gm, unit 2c), overlying thrust sheet N. In the top of the footwall block below the thrust fault the planar bedded coarse-grained gravel (Gm) is deformed by smaller reverse faults to form an imbricate stack between points 455 and 470 m in the profile.

The hanging-wall anticline of thrust sheet F is exposed at 170–210 m in the cliff section (Fig. 2). The anticline formed as the thrust sheet F was displaced about 30 m up along the footwall ramp and over the flat at the back of thrust sheet E (Fig. 6). Thrust sheet F is *c.* 18 m thick and comprises unit 1 overlain by a succession of unit 2a–2e. Unit 1 is intersected by vertical fissures, and in the foreland-dipping limb of the hanging-wall anticline small-scale thrusts cut the upper contact of unit 1 (Fig. 2). The thrust fault is recognised in the glaciofluvial sediments by a dislocated layer of gravel (unit 2c) between points 140 m and 160 m. During thrusting small decimetre-scale reverse faults formed in the sand (unit 2d) above the gravel layer (Fig. 2). Just above the thrust fault at point 160 m isolated gravel layers (unit 2c) are seen lying almost vertical in the sandy unit (unit 2d) (Fig. 2). The sand and gravel pockets are interpreted to constitute the core of an upright anticline of the glaciofluvial clay and silt (unit 2e) disturbed by hydrodynamic mobilisation due to increased compression during translation (Fig. 6).

The *c.* 14 m thick thrust sheet G consists of unit 1 followed by a glaciofluvial succession of unit 2a and unit 2c–2e. The frontal edge of thrust sheet G is truncated by a glaciotectionic unconformity (Fig. 6). The thrust sheet was displaced at least 25 m on top of the footwall of thrust sheet F. During displacement a small hanging-wall anticline (seen at point 240 m in Fig. 2) formed above a hanging-wall ramp (Fig. 6). Furthermore, a local imbricate fan of gravel with at least four reverse faults formed within the footwall (seen at point 220 m) (Fig. 2). Along the upper hanging-wall flat an intrusion of massive gravel (9 m in length) is observed in unit 1 (Fig. 7a) which, facilitated by high pore-water pressure, was injected during stress propagation. Thrust sheet G is truncated by thrust sheet H whose frontal edge consisting of a glaciofluvial succession of unit 2c–2e is exposed at point 260 m (Fig. 2). It is estimated that thrust sheet H was displaced approximately 8 m, which caused the overturned folding of the horizontally bedded gravel and sand (unit 2c and 2d). An erosional unconformity cuts the tip of the hanging-wall of the thrust sheet upon which unit 3 was deposited (Fig. 6).

In the lower part of the 280–350 m section the cliff exposure is limited. However, based on variation in bedding directions and the presence of unit 1 between points 280 m and 290 m and its recurrence at point 320 m (Fig. 2), it is inferred that this cliff section contains three thrust sheets – thrust sheet I, J and K (Fig. 6). All three thrust sheets are composed of unit 1 succeeded by a succession of unit 2c–2e. Both thrust sheets I and J are estimated to have been displaced about 8 m along the thrust faults, whereas thrust sheet K seems

only to have been displaced 2 m. At point 320 m the hanging-wall of thrust sheet J is cut by a reverse fault along which a fault-propagation fold formed within the gravel (unit 2c) (Fig. 6). Displacement along this reverse fault was less than 1 m. The three thrust sheets and thrust sheet L are truncated by an erosional unconformity whereupon unit 4 was deposited (Fig. 6). Both unit 3 and unit 4 are interpreted to have been deposited in a piggyback basin, here designating a local depositional basin wherein sediments are syn-tectonically accumulated on the back of translating thrust sheets (Pedersen 2005).

Thrust sheet L is composed of unit 1 and a succession of unit 2a and unit 2c–2e. At the frontal edge, the thrust sheet developed into a major diapir (between points 380 m and 410 m in Fig. 2). The diapir formed as the lower part of the till (unit 1) became mobilised and intruded the overlying boulder (unit 2a) and gravel beds (unit 2c), causing the undulation of these layers (Pedersen 2005). The compressional deformation was here released in hydrodynamic brecciation, and displacement along the thrust fault only amounted to 2 m. In the crest of thrust sheet L open, inclined folds as well as recumbent folds are observed within the glaciofluvial succession of clay and silt (unit 2e) between point 420 m and 440 m. A fold axis of $319^{\circ}/9^{\circ}$ was constructed from an overturned fold outlined in a *c.* 0.5 m thick sand layer interbedded in unit 2e (Fig. 7b). This fold axis direction indicates compressive stress from NE. At the trailing end, thrust sheet L is folded into a footwall syncline (Fig. 6).

The approximately 17 m thick thrust sheets M and N consist of unit 1 overlain by unit 2a–2e. Possibly, thrust sheets M and N initially constituted one thrust sheet but became internally divided by the thrust fault at point 460 m at a late stage in the deformation. The tip of the thrust fault separating the two sheets is refracted into parallelism with the bedding in unit 2e, which tends to make thrust sheet M a duplex structure below thrust sheet N (Fig. 6). The two thrust sheets are displaced along a blind thrust fault that terminates beneath the succession of glaciofluvial clay and silt (unit 2e). Thrusting was first initiated by the propagation of thrust sheet M along a fault plane dipping 39° ENE. A hanging-wall anticline (seen between points 450 m and 480 m in Fig. 2) formed as thrust sheet M was displaced about 8 m. As thrust sheet N was displaced about 2 m along the *c.* 30° dipping thrust fault, the underlying sediments were folded into a footwall syncline where the planar sand (unit 2d) was tilted vertically in the northern limb (Fig. 2). In the hanging-wall of thrust sheet N a local imbricate fan formed with more than four reverse faults in the gravel beds of unit 2c and 2d. One of these reverse faults can be traced to continue down into the underlying unit 1

dipping 44° NE (Fig. 2). The reverse faults are therefore interpreted to have been formed by multiple small-scale up-thrusts of unit 1.

Thrust sheet O is c. 18 m thick and, judged from the scarce exposure, is interpreted to comprise unit 1 overlain by unit 2c and likely unit 2d. During propagation unit 1 became wedge-shaped because of ramping (Fig. 7c). Furthermore, a small hanging-wall anticline formed above the hanging-wall ramp seen at point 500 m (Fig. 2). The frontal part of the hanging-wall thrust sheet O is truncated by a glaciotectionic unconformity (Fig. 6). Within the hanging-wall divergent bedding directions suggest that a thrust fault developed in the gravel layer, causing a local thickening of the succession. It is estimated that thrust sheet O was displaced at least 30 m.

In the cliff section at 520–680 m only the upper part of the cliff is exposed. The inferred thrust sheets in this section are, therefore, somewhat uncertain. For both thrust sheet P and Q there is no direct evidence of a thrust fault. Thrust sheet P is defined on the basis of divergent bedding directions within the layer of gravel (unit 2c), while thrust sheet Q is determined from the divergent bedding directions within the glaciofluvial sand (unit 2d) and clay/silt (unit 2e) (Fig. 2). In the hanging-wall of thrust sheet Q the horizontally bedded clay and silt of unit 2e seems generally undisturbed, whereas in the footwall of thrust sheet P unit 2d has been subjected to ductile deformation. The folds observed within unit 2e likely formed during propagation of thrust sheet Q. The deformed succession of unit 2e is discordantly overlain by unit 4 (Fig. 2). It is estimated that thrust sheets P and Q are c. 30 m thick and were displaced 25 m and 13 m, respectively.

To the north, thrust sheet Q is overlain by thrust sheet R. This thrust sheet comprises unit 1 and a glaciofluvial succession of unit 2c–2d and was displaced c. 15 m up along the footwall ramp on thrust sheet Q. Thrust sheet R was presumably affected by diapirism which has caused the trailing end to dip upward (Fig. 6). Diapirism probably dominated the cliff section between point 710 m and 840 m. In the two-dimensional drawing by Jessen (1930, 1935) the northern part of the cliff is dominated by glaciofluvial sediments with only a few traces of the lower till, whereas the drawing by Frederiksen (1976) shows a greater extent of the lower till, which is even greater in the current study. Frederiksen (1975) attributed this change in material to erosion gradually stripping away material from an upright anticline consisting of units 1 and 2. The fold likely formed because of diapirism as the mobilised till (unit 1) intruded into the overlying glaciofluvial succession (unit 2a–2e) and thereby caused the folding of these layers.

Structural framework and balancing of the thrust-fault complex

The cross section of the glaciotectionic complex is approximately 900 m long. The complex contains at least eighteen, generally 15–20 m thick thrust sheets displaced along thrust faults dipping 30–40° NNE. No thrust faults are observed in the northernmost part of the cliff face between points 720 m and 920 m, but the cliff section is partly obscured by scree. Diapirism is, though, interpreted to have played an important role in this part of the complex.

The thrust faults are rooted in a basal décollement plane estimated at around 20 m below sea level (Fig. 6). The upturned ends of the thrust sheets would have formed the ridges of the thrust-fault complex. On the up-glacier side of the ridges depressions formed, resulting in piggyback basins wherein units 3 and 4 were deposited.

The architecture of the glaciotectionic complex is dominated by thrust faults with a ramp-flat geometry whereby a hanging-wall flat is displaced on top of a footwall ramp. Thrust sheet F, however, is inferred to have been displaced along a thrust fault with a ramp-flat-ramp geometry. The hanging-wall of thrust sheet F was thrust up along a lower footwall ramp, translated along the intermediate footwall flat of thrust sheet E and finally displaced up along the upper footwall ramp. During propagation over the lower footwall ramp-hinge the hanging-wall was folded into an anticline with a foreland-dipping forelimb and a hinterland-dipping backlimb. Hanging-wall anticlines have also been observed above the hanging-wall ramps of thrust sheets E, G and O which were likewise formed by the folding of the hanging-wall as it propagated over the ramp-hinge.

At the trailing end of thrust sheets C, L and M, footwall synclines formed beneath the footwall ramps. The synclines formed because the tip of the thrust sheets became folded as the hanging-walls were thrust up along the ramps. Continued propagation resulted in the thrust faults breaking through the folded layers and separating the fold so that a syncline formed below the thrust faults and an anticline above, thereby causing the tilting of the horizontally bedded strata towards the thrust faults.

On the basis of two-dimensional mapping of the cliff section we estimate that the thrust sheets were displaced at least 235 m (the sum of displacement for all the thrust sheets). The restored length of the complex (the lateral extension of deposits prior to deformation) is therefore at least 955 m as the length of the thrust-fault complex is calculated to be 720 m. The

cliff section between points 720 m and 920 m is omitted because the presence of thrust faults in this part of the cliff is unknown. The glaciotectonic shortening of the foreland can be calculated using the formula by Croot (1988) whereby Shortening = (change in length/restored length) $\times 100$. Accordingly, we estimate that the complex has undergone a shortening of least 24% as a result of the deformation.

Glaciodynamic stratigraphy

Based on the glaciodynamic stratigraphy proposed by Pedersen (1996), the sediments and the glaciotectonic deformation in the Halk Hoved cliff section represent three glaciodynamic events which correspond to three glaciodynamic sequences.

The first glaciodynamic sequence is represented by units 1 and 2. In previous studies, Houmark-Nielsen (1987, 2007) correlated unit 1 to the Lillebælt Till Formation deposited during the Warthe glaciation in Late Saalian. The glaciers advanced through the Baltic depression from easterly directions, and the Lillebælt Till Formation is therefore characterised by a pronounced Baltic clast provenance (Houmark-Nielsen 1987, 2007) with a high content of both Cretaceous–Danian limestone and Palaeozoic limestone (Fig. 3).

On top of the Lillebælt Till Formation the fining-upward succession of glaciofluvial sediments (unit 2a–2e) was deposited. In the current investigation, the glaciofluvial sediments are shown to petrographically deviate from the underlying Lillebælt Till Formation by having a lower content of crystalline rocks and a higher content of quartz (Fig. 3). The difference in the petrographical composition could indicate that unit 2 was not deposited by the same ice advance as unit 1. The glaciofluvial sediments were estimated to be of Weichselian age based on studies of similar deposits overlying Eemian material (Houmark-Nielsen 1987). However, OSL (Optically Stimulated Luminescence) dates show ages between 169 and 167 kyr (Houmark-Nielsen 2007), indicating that the glaciofluvial succession, like the Lillebælt Till Formation, most probably was deposited during the Warthe glaciation. If so, then the petrographical deviation must be the result of the difference in the depositional processes as the two units represent two different depositional environments; a subglacial environment and a glaciofluvial environment.

The second glaciodynamic sequence represents the large-scale deformation of units 1 and 2 followed by the syntectonic deposition of units 3 and 4. The structural analysis of the glaciotectonic structures showed that the sediments were primarily deformed

by glacial stress from N-NE. The sediments are, therefore, interpreted to be deformed by the NE advance in Late Weichselian, which is consistent with previous studies (Frederiksen 1975; Houmark-Nielsen 1987). During deformation piggyback basins formed, resulting in syntectonic deposition of units 3 and 4. The petrographical composition of unit 3 shows a strong resemblance to that of the underlying glaciofluvial sediments (unit 2) (Fig. 3). Unit 3 is interpreted to have been deposited by a hyperconcentrated flow, which was generated by the mobilisation of water-saturated material down the back of thrust sheet G. The primary source of material would have been the glaciofluvial sediments of unit 2, and unit 3 therefore inherited the petrographical composition of unit 2.

In contrast to units 2 and 3, unit 4 has a high content of crystalline rocks and a low content of quartz (Fig. 3). In previous investigations unit 4 was interpreted as a subglacial till (Jessen 1930; Frederiksen 1976) and petrographically correlated to the Mid Danish Till Formation deposited by the NE advance in Late Weichselian (Houmark-Nielsen 1987, 2007). Although unit 4 in the current study is interpreted as a glaciolacustrine diamict, it is possible that the Mid Danish Till Formation may be present at Halk Hoved because unit 4 between points 490 m and 560 m was not examined up-close. At point 330 m a sample from the upper part of unit 4 (S4.7; Fig. 2) has a different petrographical composition compared to the rest of the samples from unit 4 (Fig. 3). The sample differs by containing a higher quantity of sedimentary rocks, Cretaceous–Danian limestone and Palaeozoic limestone, while the content of flint is very low. This petrographical deviation could indicate that this part of unit 4 was deposited by another ice advance, possibly the Young Baltic advance, because the high content of sedimentary rocks and Palaeozoic limestone suggests a Baltic origin. However, in the current study it is not possible to ascertain whether this deviating sample represents a different glaciation or depositional environment than the rest of unit 4.

The whole assemblage of units 1–4 constitutes one glaciotectonic unit. The complex is truncated by a glaciotectonic unconformity, formed as the NE advance finally overrode and eroded the upper part of the thrust-fault complex.

The third glaciodynamic sequence is represented by units 5 and 6. The discontinuous glaciofluvial succession (unit 5) was deposited on top of the glaciotectonic unconformity. It is overlain by unit 6 (till) that petrographically correlates to the East Jylland Till Formation (Houmark-Nielsen 1987, 2007) deposited by the Young Baltic advance in Late Weichselian. The Young Baltic advance transgressed through the Baltic depression, and its deposits should therefore be char-

acterised by a high content of Palaeozoic limestone. The fact that no Cretaceous–Danian limestone or Palaeozoic limestone have been observed in unit 6 could presumably be due to weathering. The glaciofluvial sediments (unit 5) were most likely also deposited by the Young Baltic ice sheet, but it is possible that it may also have been deposited by the NE advance during its retreat from the MSL.

Factors controlling the glaciotectonic deformation

In order for proglacial deformation to occur, the compressive stress imposed on the foreland by the ice sheet must exceed the strength of the weakest sediment within the substratum. Several studies of both modern and ancient glaciotectonic complexes (Aber *et al.* 1989; Pedersen 1996, 2005; van der Wateren 1995, 2005) have shown that the presence of fine-grained material (*e.g.* Tertiary marine clay and silts, glacial and interglacial lacustrine fine-grained sediments or marine clay and silts) is often a precondition for the development of large-scale proglacial deformation. At the 1 km long coastal cliff of Ristinge Klint, the décollement plane developed within marine Cyprina Clay which, facilitated the stacking of more than thirty up to 20 m thick thrust sheets (Aber *et al.* 1989; Kristensen *et al.* 2000). Similarly, the formation of multiple thrust sheets and nappes at the 6 km long costal cliff of Rubjerg Knude was facilitated by glaciolacustrine clay (Lønstrup Klint Formation), resulting in a 50% glaciotectonic shortening of the substratum (Pedersen 2005). In both cases the fine-grained layer, assisted by high pore-water pressures, acted as a low-friction plane along which the thrust sheets were easily displaced.

In the investigation by Frederiksen (1975), as well as in the current study, no evidence of such a fine-grained layer acting as a low-friction sliding plane was found at Halk Hoved. In this area the pre-Quaternary surface is situated well below the décollement plane, and Tertiary clay is therefore excluded as a potential contributor to failure.

If the lithology is less favourable to deformation, such as in the absence of a fine-grained layer, then the formation of a décollement plane is strongly dependent upon the hydrogeology of the foreland. Simulations of groundwater flow beneath past ice sheets show that groundwater generally flows downwards beneath the ice sheet and upwards at the ice margin and in the proglacial zone (Boulton & Caban 1995; Piotrowski 1997a, b; Carlson *et al.* 2007; Person 2007). When an aquifer in the proglacial zone is overlain by a low-conductivity layer (*e.g.* till or permafrost), the

upward flow will cause water pressures to build up in the aquifer. If such an aquifer is loaded sufficiently rapidly by an ice sheet, preventing gradual pressure dissipation, the elevated pore-water pressures can cause hydrofractures and liquefaction/dilation in the overlying sediments (Boulton & Caban 1995). Liquefaction/dilation occurs as the high water content weakens the electrostatic bonds and increases the distance between the individual grains, thereby reducing the shear strength of the sediment. As shear stress is applied to the liquefied/dilated sediment, the mixture of water and sediment would initiate flow (Evans *et al.* 2006), so that during thrusting the mixture would act as a lubricant creating a plane of low resistance whereupon the thrust sheet is easily displaced (Strayer *et al.* 2001; Philips *et al.* 2008).

In the substratum adjacent to Halk Hoved the Lillebælt Till Formation (unit 1) is estimated to be more than 10–15 m thick (Houmark-Nielsen 2007). In a few well logs approximately 3 km west of Halk Hoved, obtained from the web-based Jupiter well log archive (GEUS 2011a), the thick Lillebælt Till Formation is observed to overlie glaciofluvial sand. Recent TEM (Transient ElectroMagnetic) surveys in the area, obtained from the web-based GERDA geophysical data archive (GEUS 2011b), show the sand layer situated in a more than 100 m deep buried valley extending from Halk Strand northeast of Hejsager and up towards Grarup and Haderslev Fjord (Fig. 1). With the present data, it is not known if the sand layer also extends eastwards into the Halk Hoved area. If it does, the décollement plane likely developed along the lithostratigraphical boundary between the sand and the till. The base of the Lillebælt Till would thus be situated at the décollement plane around 20 m below sea level, which is in accordance with the thickness estimate of Houmark-Nielsen (2007).

The formation of modern glaciotectonic complexes is often associated with the presence of permafrost (Hambrey & Huddart 1995; Boulton *et al.* 1999). As mentioned above, permafrost may be conducive to proglacial deformation as it may facilitate high groundwater pressures. Permafrost, furthermore, hardens the sediments so that the compressive stress applied by the ice sheet can be transmitted horizontally over a large area. However, some authors (Croot 1987, 1988; van der Wateren 2005) emphasise that permafrost is not crucial in the formation of large thrust-fault complexes. In the southern part of Jutland periglacial conditions dominated throughout Weichselian and were only interrupted by the Ristinge ice advance in Middle Weichselian and the NE advance with its successive readvances in Late Weichselian (Houmark-Nielsen 2007). It is possible that prior to deformation permafrost was present as the ice sheet

advanced from NE towards the MSL, but in the current investigation there is no sedimentary evidence of permafrost.

Formation of the thrust-fault complex

The thrust-fault complex was formed by proglacial glaciotectonic deformation caused by the NE advance in Late Weichselian. The foreland would have consisted of a fining-upward glaciofluvial succession (unit 2) overlying a thick till layer (unit 1), which in turn rested on an aquifer. As the ice sheet advanced towards the area, basal meltwater would have been partly drained through the substratum generating glacially driven groundwater flow in the aquifer beneath the till layer. In front of the ice margin the high groundwater pressures beneath the till triggered its oversaturation and drop of shear strength. Thrust faults developed as the lateral stresses within the foreland, generated primarily by the weight of the ice sheet (known as gravity spreading; cf. Huuse & Lykke-Andersen 2000; Bennett 2001), exceeded the shear strength of the till. As a thrust sheet formed it was pushed up along the fault plane facilitated by liquefaction/dilation in the lower part of the till. In some areas the dilation of the till mass resulted in diapirism as seen in thrust sheet K and to a more extensive degree in the northernmost part of the cliff between points 700 m and 920 m (Fig. 6).

A new thrust sheet usually developed in the foot-wall of an older thrust sheet so that the older thrust sheets would be carried forward on the backs of the younger ones, which is known as piggyback thrusting analogous to thin-skinned tectonics within orogenic belts (cf. Suppe 1985). The sequence of thrust sheets, therefore, started with thrust sheet R and ended with thrust sheet A. However, two of the thrust sheets, E and N, formed in the hanging-wall of pre-existing thrust sheets, D and M, because of the development of internal thrust faults. Thrust sheet propagation along the thrust faults ranged between 1 m and 30 m, which is low compared to other thrust-dominated complexes such as Rubjerg Knude and Ristinge Klint. The reason for this difference may be the fact that the faults developed in till and not in fine-grained material. The till, even though dilated/liquefied, would likely have been more resistant to sliding during propagation because of the higher frictional strength of the till compared to fine-grained sediments such as marine clay and glaciolacustrine clay.

During deformation piggyback basins formed, giving rise to proglacial ponds collecting meltwater and

sediment. A larger basin formed between thrust sheets G and O, wherein syntectonic deposition of units 3 and 4 occurred. The tip of thrust sheet G created a ridge with glaciofluvial sediments on the up-glacier side. High pore-water pressures within the glaciofluvial sediments, and gravity, caused the material to slide down the ridge into the piggyback basin generating a hyperconcentrated flow of predominantly gravel, sand and silt (unit 3). In the water-filled basin glacial diamicton (unit 4) was deposited by debris rainout from floating icebergs. After the piggyback basins became filled by sediment, the NE advance overrode the glaciotectonic complex and truncated its upper part, smoothing the geomorphological expression of the complex.

Conclusions

The history of the glaciotectonic complex at the coastal cliff of Halk Hoved comprises three major ice advances during the late Saalian and late Weichselian glaciations. In Late Saalian, the Warthe ice sheet advanced from easterly directions through the Baltic region and deposited the Lillebælt Till Formation (unit 1). During the retreat, a fining-upward succession of glaciofluvial sediments (unit 2a–2e) was deposited. Following a long ice-free period, the advance of the late Weichselian ice sheet from the northeast triggered prominent proglacial deformation and a thrust-fault complex formed, extending for *c.* 700 m in front of the ice margin. The glaciotectonic complex comprises at least eighteen *c.* 15–20 m thick thrust sheets stacked by piggyback thrusting. Accumulated displacement amounts to at least 235 m, resulting in at least 24% shortening of the complex. Failure is suggested to be due to elevated pore-water pressure in a confined sand aquifer beneath the Lillebælt Till Formation. The high pore-water pressures resulted in dilation/liquefaction which reduced the shear strength of the till and a décollement plane formed along the lithostratigraphical boundary between the Lillebælt Till Formation and the underlying aquifer. The décollement plane is estimated to be situated about 20 m below sea level. During deformation, piggyback basins formed between the thrust sheets, wherein a sediment of hyperconcentrated flow (unit 3) and glaciolacustrine diamicton (unit 4) were syntectonically deposited. The complex is truncated by a glaciotectonic unconformity, formed as the NE advance finally overrode and eroded the upper part of the thrust-fault complex. Following an ice-free phase, a glaciofluvial succession (unit 5) and the East Jylland Till Formation (unit 6) were deposited by the Young Baltic ice stream as it advanced

from southeast through the Baltic region. The Halk Hoved glaciotectionic complex illustrates the nature of the interactions between the Weichselian Ice Sheet and its soft beds, in particular the role of localized sediment deformation triggered by elevated subglacial pore-water pressures close to the ice sheet periphery.

Acknowledgements

We thank the technicians at the Department of Geoscience, Aarhus University for their help with laboratory analyses, Jette Sørensen (VIA University College, Horsens) for discussions and comments on the first draft of this paper, and Rud Friberg (Sønderjylland Amt) for discussions and support. Journal referees Stig A. Schack Pedersen and Michael Houmark-Nielsen are thanked for their thorough and constructive reviews which considerably improved the paper.

Dansk sammendrag

Størstedelen af de kortlagte glacialtektoniske komplekser i Danmark blev dannet under fremrykningen af de store skandinaviske gletschere i Weichsel. Isens fremadrettede tryk på underlaget forårsagede folding og oppresning af sedimenterne i flager, der blev stablet oven på hinanden. Langs den ca. 900 m lange og 10–20 m høje kystklint Halk Hoved, der er beliggende ca. 12 km sydøst for Haderslev i den sydlige del af Jylland, ses et smukt og velblottet eksempel på et glacialtektonisk kompleks primært opbygget af skråtstillede flager.

I en strukturgeologisk og sedimentologisk undersøgelse af klinten er der udarbejdet et geologisk tværsnit, som viser den overordnede struktur af de glacialtektoniske deformationer samt udbredelsen af de enkelte lithofacies. Lagserien er på baggrund af de sedimentologiske karakteristika samt kornstørrelses- og fingerusanalyser inddelt i seks lithostratigrafiske enheder. Den nederste lithostratigrafiske enhed (unit 1) udgøres af en mindst 4 m tyk, leret till, som henføres til Lillebælt Till Formationen afsat i forbindelse med Warthe fremstødet i Sen Saale. Tillen overlejres af en ca. 6–12 m tyk smeltevandssekvens (unit 2), hvis kornstørrelse aftager opefter. Smeltevandssekvensen tolkes som repræsenterende en ændring i det glaciofluviale miljø fra en proximal til distal flodslette som følge af tilbagesmeltingen af Warthe fremstødet i Sen Saale.

Både Lillebælt Till Formationen og den overliggende smeltevandssekvens blev udsat for proglacial de-

formation i forbindelse med Nordøst (NØ) fremstødet i Sen Weichsel. Det foreslås, at deformationen skyldes forhøjet porevandstryk i underlaget. Under fremrykningen steg vandtrykket i sandlag under Lillebælt Till Formationen, og gradientforholdene blev opadrettede. Dette førte til et forhøjet porevandstryk i tillens nedre del. Isens fremadrettede tryk på underlaget samt det forhøjede porevandstryk resulterede i dannelsen af forkastninger hældende 30–40° NNØ, forbundet af "et décollementplan" (LML) langs laggrænsen mellem grundvandsmagasinet og tillen. Stedvis førte det forhøjede porevandstryk også til diapirisme, hvori den vandmættede till trængte op i de overliggende sedimenter.

Langs forkastningerne blev mindst 18 ca. 15–20 m tykke flager forskudt i en størrelsesorden af 1–30 m. De blev stablet oven på hinanden via piggyback overskydning, hvori de yngste flager blev forskudt under den samlede vægt af tidligere dannede overskydningsflager. Der har i alt været en samlet forskydning på ca. 240 m svarende til en glacialtektonisk afkortning af landskabet på ca. 24%.

Diskordant over de deformerede sedimenter, ses en 1–5 m tyk, siltet-sandet diamicton (unit 3) med enkelte indslag af sorteret materiale. Enheden tolkes at være aflejret af en hyperkoncentreret sedimentstrøm, der opstod ved en mobilisering af smeltevandssedimenterne (unit 2) ned langs ryggen af en glacialtektonisk flage. Enhed 3 er overlejret af en 2–13 m tyk, siltet-leret diamicton (unit 4) tolket som aflejret i en issø foran NØ fremstødet. Både enhed 3 og 4 tolkes som syntektonisk aflejret i et piggyback bassin, dvs. et bassin beliggende ovenpå og mellem de glacialtektoniske flager.

Hele sekvensen af sedimenter er afskåret af en glacialtektonisk inkonformitet og diskordant overlejret af en diskontinuert, 1–4 m tyk smeltevandssekvens. Toppen af klinten er dækket af en 1–2 m tyk, leret till, der tilhører East Jylland Till Formationen. Begge enheder er afsat af det Ungbaltiske fremstød i Sen Weichsel.

References

- Aber, J.S., Croot, D.G. & Fenton, M.M. 1989: Glaciotectionic landforms and structures. Kluwer Academic Publisher, Dordrecht, Netherlands, 200 pp.
- Benn, D.I. 1996: Subglacial and subaqueous processes near a glacier grounding line: sedimentological evidence from a former ice-dammed lake, Achnasheen, Scotland. *Boreas* 25, 23–36.
- Bennett, M.R. 2001: The morphology, structural evolution and significance of push moraines. *Earth-Science Reviews* 53, 197–236.

- Bennett, M.R., Huddart, D. & Thomas, G.S.P. 2002: Facies architecture within a regional glaciolacustrine basin: Copper River, Alaska. *Quaternary Science Reviews* 21, 2237–2279.
- Beverage, J.P. & Culbertson, J.K. 1964: Hyperconcentrations of suspended sediment. *Proceedings of the American Society of Civil Engineers, Journal of the Hydraulics Division* 90, 117–128.
- Bilka, L.H. & Nemec, W. 1998: Postglacial colluvium in western Norway: depositional processes, facies and Palaeoclimatic record. *Sedimentology* 45, 909–959.
- Boulton, G.S. 1978: Boulder shapes and grain-size distributions of debris as indicators of transport paths through a glacier and till genesis. *Sedimentology* 25, 773–799.
- Boulton, G.S. & Caban, P. 1995: Groundwater flow beneath ice sheets: part II – its impact on glacier tectonic structures and moraine formation. *Quaternary Science Reviews* 14, 563–587.
- Boulton, G.S., van der Meer, J.J.M., Beets, D.J., Hart, J.K. & Ruegg, G.H.J. 1999: The sedimentary and structural evolution of a recent push moraine complex: Holmstrømbreen, Spitsbergen. *Quaternary Science Reviews* 18, 339–371.
- Brandes, C. & Le Heron, D. 2010: The glaciotectionic deformation of Quaternary sediments by fault-propagation folding. *Proceedings of the Geologists' Association* 121, 270–280.
- Carlson, A.E., Jenson, J.W. & Clark, P.U. 2007: Modeling the subglacial hydrology of the James Lobe of the Laurentide Ice Sheet. *Quaternary Science Reviews* 26, 1384–1397.
- Croot, D.G. 1987: Glacio-tectonic structures: a mesoscale model of thin-skinned thrust sheets? *Journal of Structural Geology* 9, 797–808.
- Croot, D.G. 1988: Morphological, structural and mechanical analysis of neoglacial ice-pushed ridges in Iceland. In Croot, D.G. (ed.): *Glaciotectonics: forms and processes*, 33–47. A.A. Balkema, Rotterdam, Netherlands.
- Domack, E.W. & Lawson, D.E. 1985: Pebble fabric in an ice-rafted diamicton. *Journal of Geology* 93, 577–591.
- Dowdeswell, J.A., Whittington, R.J. & Marienfeld, P. 1994: The origin of massive diamicton facies by iceberg rafting and scouring, Scoresby Sund, East Greenland. *Sedimentology* 41, 21–35.
- Dreimanis, A. & Vagners, U.J. 1971: Bimodal distribution of rock and mineral fragments in basal tills. In: Goldthwait (ed.): *Till, a Symposium*, 237–250. Ohio State University Press.
- Ehlers, J. 1979: Fine gravel analyses after the Dutch method as tested out on Ristinge Klint, Denmark. *Bulletin of the Geological Society of Denmark* 27, 157–165.
- Evans, D.J.A., Philips, E.R., Hiemstra, J.F. & Auton, C.A. 2006: Subglacial till: Formation, sedimentary characteristics and classification. *Earth-Science Reviews* 78, 115–176.
- Evenson, E.B., Dreimanis, A. & Newsome, J.W. 1977: Subaquatic flow tills: a new interpretation for the genesis of some laminated till deposits. *Boreas* 6, 115–133.
- Frederiksen, J.K. 1975: Glaciale tektoniske og -stratigrafiske undersøgelser i udvalgte områder i det sydlige Danmark. Prisopgave, University of Copenhagen, 170 pp.
- Frederiksen, J.K. 1976: Hvad de Sønderjyske klinger fortæller. *VARV* 2, 35–45.
- GEUS 2011a: Danmarks og Grønlands Geologiske Undersøgelse, Jupiter boredatabase. <http://Jupiter.geus.dk>.
- GEUS 2011b: Danmarks og Grønlands Geologiske Undersøgelse, Jupiter geofysiske database. <http://gerda.geus.dk/Gerda/>.
- Haldorsen, S. 1981: Grain-size distribution of subglacial till and its relation to glacial crushing and abrasion. *Boreas* 10, 91–107.
- Haldorsen, S. 1983: Mineralogy and geochemistry of basal till and their relationship to till-forming processes. *Geografisk Tidsskrift* 63, 15–25.
- Hambrey, M.J. & Huddart, D. 1995: Englacial and proglacial glaciotectionic processes at the snout of a thermally complex glacier in Svalbard. *Journal of Quaternary Science* 10, 313–326.
- Houmark-Nielsen, M. 1987: Pleistocene stratigraphy and glacial history of the central part of Denmark. *Bulletin of the Geological Society of Denmark* 36, 1–189.
- Houmark-Nielsen, M. 2007: Extent and age of Middle and Late Pleistocene glaciations and periglacial episodes in southern Jylland, Denmark. *Bulletin of the Geological Society of Denmark* 55, 9–35.
- Huuse, M. & Lykke-Andersen, H. 2000: Large-scale glaciotectionic thrust structures in the eastern Danish North Sea. *Geological Society, London, Special Publications* 176, 293–305.
- ICS, International Commission on Stratigraphy 2010: Regional chronostratigraphical correlation table for the last 270,000 years, Europe north of the Mediterranean. http://www.stratigraphy.org/upload/Quaternary_last270ka.pdf.
- Jakobsen, P.R. 1996: Distribution and intensity of glaciotectionic deformation in Denmark. *Bulletin of the Geological Society of Denmark* 42, 175–185.
- Jakobsen, P.R. 2003: GIS based map of glaciotectionic phenomena in Denmark. *Geological Quarterly* 47, 331–338.
- Jessen, A. 1930: Klinten ved Halk Hoved. *Danmark Geologiske Undersøgelse*, VI Række 8, 26 pp.
- Jessen, A. 1935: Beskrivelse til geologisk kort over Danmark. *Kortbladet Haderslev. Danmark Geologiske Undersøgelse*, I Række 17, 95 pp.
- Kjær, K.H., Houmark-Nielsen, M. & Richardt, N. 2003: Ice-flow patterns and dispersal of erratics at the southwestern margin of the last Scandinavian Ice Sheet: signature of palaeo-ice streams. *Boreas* 32, 130–148.
- Kristensen, P., Gibbard, P., Knudsen, K.L. & Ehlers, J. 2000: Last Interglacial stratigraphy at Ristinge Klint, South Denmark. *Boreas* 29, 103–116.
- Kronborg, C. 1986: Fine-gravel content of tills. In: Møller, J.T. (ed.), *Twentyfive Years of Geology in Aarhus*. Aarhus University, *Geoskrifter* 24, 189–210.
- Kronborg, C., Bender, H., Bjerre, R., Friberg, R., Jacobsen, H.O., Kristiansen, L., Rasmussen, P., Sørensen, P.R. & Larsen, G. 1990: Glacial stratigraphy of East and Central Jutland. *Boreas* 19, 273–287.

- Krüger, J. & Kjær, K.H. 1999: A data chart for field description and genetic interpretation of glacial diamicts and associated sediments – with examples from Greenland, Iceland and Denmark. *Boreas* 28, 386–403.
- Larsen, N.K., Piotrowski, J.A. & Kronborg, C. 2004: A multi-proxy study of a basal till: a time-transgressive accretion and deformation hypothesis. *Journal of Quaternary Science* 19, 9–21.
- May, R.W. 1977: Facies model for sedimentation in the glaciolacustrine environment. *Boreas* 6, 175–180.
- Miall, A.D. 1985: Architectural-element analysis: a new method of facies analysis applied to fluvial deposits. *Earth-Science Reviews* 22, 261–308.
- Mulder, T. & Alexander, J. 2001: The physical character of subaqueous sedimentary density flows and their deposits. *Sedimentology* 48, 269–299.
- Pedersen, S.A.S. 1996: Progressive glaciotectionic deformation in Weichselian and Palaeogene deposits at Feggekklit, northern Denmark. *Bulletin of the Geological Society of Denmark* 42, 153–174.
- Pedersen, S.A.S. 2005: Structural analysis of the Rubjerg Knude Glaciotectionic Complex, Vendsyssel, northern Denmark. *Geological Survey of Denmark and Greenland Bulletin* 8, 192 pp.
- Person, M., McIntosh, J., Bense, V. & Remenda, V.H. 2007: Pleistocene hydrology of North America: The role of ice sheets in reorganizing groundwater flow systems. *Reviews of Geophysics* 45, RG3007, doi: 10.1029/2006RG000206.
- Phillips, E., Lee, J.R. & Burke, H. 2008: Progressive proglacial to subglacial deformation and syntectonic sedimentation at the margins of the Mid-Pleistocene British Ice Sheet: evidence from north Norfolk, UK. *Quaternary Science Reviews* 27, 1848–1871.
- Piotrowski, J.A. 1992: Till facies and depositional environments of the upper sedimentary complex from the Stohler Cliff, Schleswig-Holstein, North Germany. *Zeitschrift für Geomorphologie Neue Folge* 84, 37–54.
- Piotrowski, J.A. 1997a: Subglacial hydrology in northwestern Germany during the last glaciation: groundwater flow, tunnel valleys, and hydrological cycles. *Quaternary Science Reviews* 16, 169–185.
- Piotrowski, J.A. 1997b: Subglacial groundwater flow during the last glaciation in northwestern Germany. *Sedimentary Geology* 111, 217–224.
- Piotrowski, J.A., Larsen, N.K., Menzies, J. & Wysota, W. 2006: Formation of subglacial till under transient bed conditions: deposition, deformation, and basal decoupling under a Weichselian ice sheet lobe, central Poland. *Sedimentology* 53, 83–106.
- Rovey, C.W. & Borucki, M.K. 1995: Subglacial to Proglacial sediment transition in a shallow ice-contact lake. *Boreas* 24, 117–128.
- Smed, P. 1981: Landskabskort over Danmark, Blad 2, Midtjylland. Geografforlaget, Brenderup, Danmark.
- Sohn, Y.K., Rhee, C.W. & Kim, B.C. 1999: Debris flow and hyperconcentrated flood-flow deposits in an alluvial fan, northwestern part of the Cretaceous Yongdong Basin, Central Korea. *Journal of Geology* 107, 111–132.
- Strayer, L.M., Hudleston, P.J. & Lorig, L.J. 2001: A numerical model of deformation and fluid-flow in an evolving thrust wedge. *Tectonophysics* 335, 121–145.
- Suppe, J. 1985: *Principles of Structural Geology*. Englewood Cliffs, Prentice Hall, New Jersey, 537 pp.
- van der Wateren, D.F.M. 1995: Structural geology and sedimentology of push moraines: processes of soft sediment deformation in a glacial environment and the distribution of glaciotectionic styles. *Mededelingen Rijks Geologische Dienst* 54, 168 pp.
- van der Wateren, D.F.M. 2005: Ice-marginal terrestrial landsystems: southern Scandinavian Ice Sheet margin. In Evans, D.J.A. (ed.): *Glacial landsystems*, 166–203. Arnold, London.